AIP | Applied Physics Letters

Mechanisms for light induced degradation in MAPbI3 perovskite thin films and solar cells

Ghada Abdelmageed, Leila Jewell, Kaitlin Hellier, Lydia Seymour, Binbin Luo, Frank Bridges, Jin Z. Zhang, and Sue Carter

Citation: Applied Physics Letters **109**, 233905 (2016); doi: 10.1063/1.4967840
View online: http://dx.doi.org/10.1063/1.4967840
View Table of Contents: http://scitation.aip.org/content/aip/journal/apl/109/23?ver=pdfcov
Published by the AIP Publishing

Mechanisms for light induced degradation in $MAPbI_3$ perovskite thin films and solar cells

Ghada Abdelmageed,[1,2,a)] Leila Jewell,[3,a)] Kaitlin Hellier,[3] Lydia Seymour,[3] Binbin Luo,[2,4] Frank Bridges,[3] Jin Z. Zhang,[2] and Sue Carter[3,b)]
[1]*Department of Radiation Physics, National Center for Radiation Research and Technology (NCRRT), Atomic Energy Authority (AEA), Nasr City, Cairo 11787, Egypt*
[2]*Department of Chemistry and Biochemistry, University of California, Santa Cruz, California 95064, USA*
[3]*Department of Physics, University of California, Santa Cruz, California 95064, USA*
[4]*College of Chemistry and Chemical Engineering, Chongqing University, Chongqing 400044, China*

(Received 11 July 2016; accepted 3 November 2016; published online 7 December 2016)

Organometal halide perovskites are highly promising materials for photovoltaic applications, yet their rapid degradation remains a significant challenge. Here, the light-induced structural degradation mechanism of methylammonium lead iodide ($MAPbI_3$) perovskite films and devices is studied in low humidity environment using X-Ray Diffraction, Ultraviolet-Visible (UV-Vis) absorption spectroscopy, Extended X-ray Absorption Fine Structure spectroscopy, Fourier Transform Infrared spectroscopy, and device measurements. Under dry conditions, the perovskite film degrades only in the presence of both light and oxygen, which together induce the formation of halide anions through donation of electrons to the surrounding oxygen. The halide anions generate free radicals that deprotonate the methylammonium cation and form the highly volatile CH_3NH_2 molecules that escape and leave pure PbI_2 behind. The device findings show that changes in the local structure at the TiO_2 mesoporous layer occur with light, even in the absence of oxygen, and yet such changes can be prevented by the application of UV blocking layer on the cells. Our results indicate that the stability of mp-TiO2-$MAPbI_3$ photovoltaics can be dramatically improved with effective encapsulation that protects the device from UV light, oxygen, and moisture. *Published by AIP Publishing.*
[http://dx.doi.org/10.1063/1.4967840]

The rapid increase in the power conversion efficiency (PCE) to above 20% of organometal halide perovskite solar cells (OMH-PSCs) has drawn significant attention of researchers;[1,2] however, the fast degradation of the material impedes their wide scale application. A number of previous studies have demonstrated the vulnerability of OMH perovskites to environmental factors such as moisture and Ultraviolet (UV) light.[3–5] Since both moisture and oxygen are easily preventable with proper encapsulation, the focus of our study is to understand the mechanisms for degradation in perovskite films and devices in a low moisture environment, with a focus on changes in the local structure.

The materials used in these experiments include N,N-dimethylformamide (DMF, spectroscopic grade, OmniSolv), 2-propanol (spectroscopic grade, Fisher Scientific), Lead iodide (PbI2, 99%, ACROS Organics, Fisher Scientific), methylammonium iodide (MAI, Dyesol), and TiO_2 nanopatricles (Solaronix). All chemicals were used as received without any further purification. The methylammonium lead iodide ($MAPbI_3$) films were prepared in air on quartz and glass slides using either the sequential deposition method or the two steps method reported elsewhere.[6,7] For the Fourier Transform Infrared (FT-IR) measurements, KBr pellets were used. The degradation process was evaluated in two different low humidity environments. In the first setup, samples were surrounded by desiccants to achieve a humidity level of <2 ppm and were aged using a 400 W metal halide lamp, with an illumination intensity of 35 (±3) mW/cm^2, at temperatures ranging between 24–32 °C. In the second setup, the samples were aged by a mercury lamp at 360 (±10) mW/cm^2 and at up to 55 °C in a nitrogen filled glove box with humidity and oxygen levels of <0.1 ppm and <10 ppm, respectively. The optical absorption spectra of the films were measured using a Jasco V-670 spectrophotometer. Fourier Transform Infrared (FT-IR) spectra were recorded with a Perkin Elmer Spectrum One FT-IR spectrophotometer. XRD analysis (XRD, Rigaku Americas Miniflex Plus powder diffractometer) was performed at a voltage of 40 kV and current of 44 mA, with a scanning angle range of 10°–60° (2θ) with a rate of 3°/min. The Pb L_{III} edge Extended X-ray Absorption Fine Structure (EXAFS) data were collected at the Stanford Synchrotron Radiation Lightsource (SSRL) on beamline 4–1 using a Si (220) double monochromator. The data were reduced using standard techniques (RSXAP),[8] converted into *k*-space, and Fourier transformed to *r*-space.

The light induced degradation of $MAPbI_3$ films was evaluated by Ultraviolet-Visible (UV-Vis) absorbance spectra in dry air and light (Figure 1, top), stored in dark dry air (Figure 1, middle), and light in N_2 filled environment (Figure 1, bottom). The fresh films spectra show the characteristic onset at 795 nm corresponding to the material's optical band gap, $E_g = 1.56$ eV, then a gradual increase up to 500 nm, and a strong PbI_2 broad absorbance in the range from 500 to 400 nm.[9] As shown in Figure 1, $MAPbI_3$ degraded only in

a)G. Abdelmageed and L. Jewell contributed equally to this work.
b)Author to whom correspondence should be addressed. Electronic mail: sacarter@ucsc.edu.

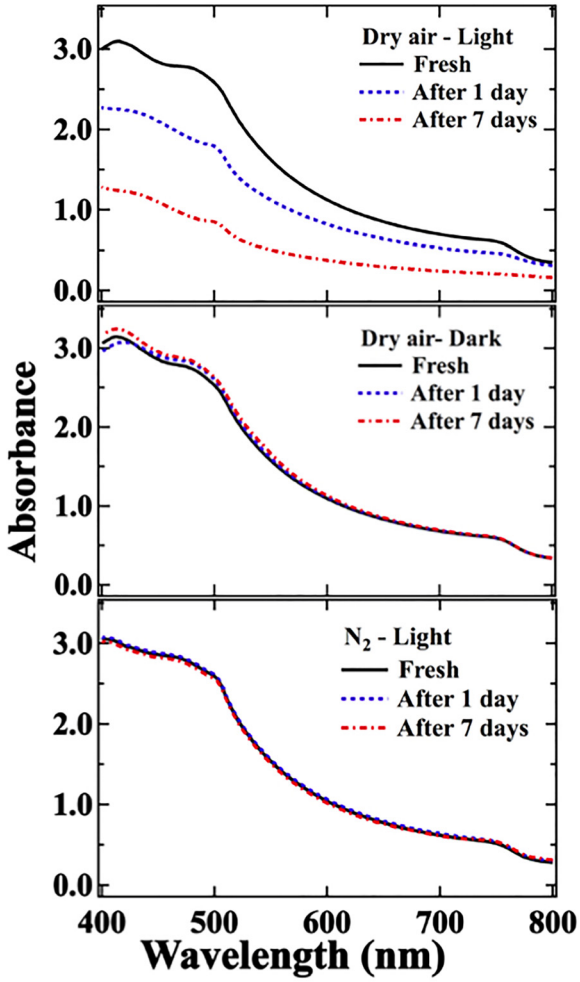

FIG. 1. UV-Vis absorbance spectra of $MAPbI_3$ films. Top: Before and after light exposure in dry air. Middle: Before and after storage in dark dry conditions. Bottom: Before and after light exposure in N_2 filled environment.

the presence of light and oxygen. As the sample degraded, the intensity of the absorbance decreased dramatically with the remaining absorption edge attributed to PbI_2. $MAPbI_3$ films were insensitive to oxygen in the dark and stable under the highly intense light with absence of oxygen, indicating that both oxygen and light are essential in the degradation mechanism. In addition, blocking UV light in the presence of oxygen did not slow down the degradation process of the $MAPbI_3$ thin films (supplementary material).

To investigate the potential changes in the organic cation during degradation, the FT-IR spectrum of the $MAPbI_3$ was evaluated after light exposure in dry air. Figure 2 shows the vibrational bands of $MAPbI_3$ fresh, and after degradation. The methyl functional groups are CH_3 rocking at 910 cm^{-1}, and C-H scissoring at 1470 cm^{-1} (Refs. 10 and 11) and the ammonium functional groups are N-H wagging at 660 cm^{-1}, NH_3 rocking at 947, 961, 1252, N-H bending at 1654 cm^{-1}, and NH_3 stretching at 3208 cm^{-1}.[11,12] A noticeable increase in intensity of the C-O stretching band at 2030 cm^{-1} was detected, as shown in Figure 2 inset,[13] indicating an interaction with photoexcited free radicals coming from the surrounding environment. In contrast, $MAPbI_3$ kept in dark for 28 days did not show any change in the peak intensities (supplementary material). In the spectra for the degraded sample

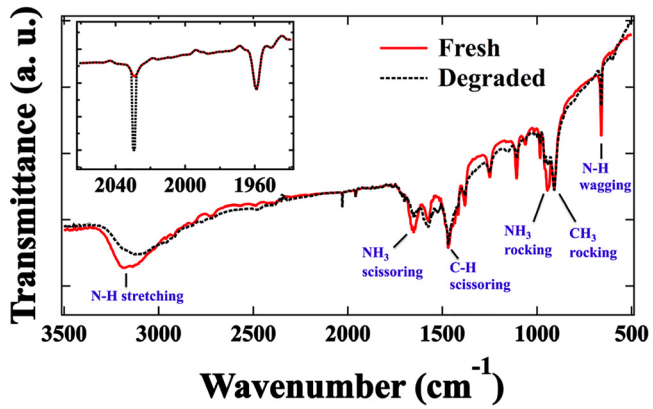

FIG. 2. FT-IR spectra of $MAPbI_3$ films, before and during light induced degradation in dry air. The decrease in the N-H bands in the degraded sample reveals a deprotonation mechanism of the ammonium group that leads to the degradation of $MAPbI_3$. Inset shows changes in the C-O stretching mode at 2030 cm^{-1} after degradation.

(Figure 2), only the peaks for the ammonium functional group diminish significantly during degradation, as observed by comparing the change in the intensity of N-H bands with respect to C-H bands before and after degradation, indicating that deprotonating NH_3 is a main step in the degradation process.

To elucidate the mechanism for the deprotonation of NH_3, a solution of MAI (10 mg/ml in isopropanol) was prepared and placed under the light. The UV-Vis absorbance spectrum of the prepared solution was recorded before and after illumination, as shown in Figure 3. The absorbance spectra show a sharp increase at the characteristic peak of complex anion tri-iodide (I_3^-) around 365 nm with continued light exposure.[14] The color of the solution changed from clear, with a light yellow tint, to intense yellow after the illumination, which indicates the release of iodine ions.[15] This change is attributed to the photoexcitation of iodide ions (I^-), which causes oxidation to the anions as in Equation (1); free electrons and iodine are released as products. In the presence of electron acceptors in the surrounding environment, such as O_2 and CO_2, the electron is transferred to form the free radicals O_2^- and CO_2^-, respectively, and the geminate recombination of the electron and the iodine in Equation (1) is hindered.[16,17] Finally, the tri-iodide anions (I_3^-) are formed in the interaction between the iodide anions and the released iodine, as in Equation (2), which appears as an increase in the intensity of the absorbance peak at 365 nm in Figure 3. Equation (2) is also reversible with the induction effect of light, as it has been reported before; with UV or visible light, the tri iodide anion dissociates into iodine molecule and iodide anion, as seen in Equation (3). The resultant iodide anion then oxidizes as in Equation (1)[14]

$$I^- \xrightarrow{h\upsilon} I + e^-, \tag{1}$$

$$I^- + I_2 \rightarrow I_3^-, \tag{2}$$

$$I_3^- \xrightarrow{h\upsilon} I^- + I_2. \tag{3}$$

The newly formed free radicals, such as the superoxide (O_2^-) and dioxidocarbonate (CO_2^-) molecules, can interact with ammonium molecules by capturing a proton to form

water (H_2O) or hydroperoxyl (HO_2) and carboxyl (HCO_2) molecules, respectively, converting them into amines. The deprotonation process was confirmed using FT-IR analysis on illuminated MAI (supplementary material, Figure S3). This analysis is also supported by a previous NMR study where the deprotonation of methylammonium iodide solution, to which potassium superoxide (KO_2) was added, was determined to be caused by the loss of a proton in the ammonium group, initiating the breakdown of $MAPbI_3$.[18] This study also revealed iodine release in toluene through the UV-Vis absorption spectrum of the fully degraded sample.

These studies indicate that the light induced degradation of $MAPbI_3$ in dry air is initiated by the iodide ions undergoing the oxidation process with the surrounding electron acceptor molecules, leading to generation of free radicals and transformation of iodine. The newly formed free radicals next deprotonate the ammonium group, converting it into amine, and bond with the released acid proton to form a stabilized molecule

$$CH_3NH_3PbI_3 \rightleftarrows PbI_2 + CH_3NH_3I, \tag{4}$$

$$2CH_3NH_3I + \frac{1}{2}O_2 \overset{h\nu}{\rightarrow} 2CH_3NH_2 + H_2O + I_2, \tag{5}$$

$$CH_3NH_3I + CO_2 \overset{h\nu}{\rightarrow} CH_3NH_2 + HCO_2 + \frac{1}{2}I_2. \tag{6}$$

Equation (4) shows the equilibrium state of $MAPbI_3$, where the lead iodide and methylammonium iodide are in interchangeable conditions with the perovskite. The methylammonium iodide interacts with free radicals, as in Equations (5) and (6). In case of superoxide (O_2^-) interaction as in Equation (5), water may be formed and contribute to the $MAPbI_3$ degradation pathway. In case of dioxidocarbonate (CO_2^-) as in Equation (6), carboxyl molecule (HCO_2) may be formed and evaporated. In either case, the methylamine (CH_3NH_2) molecule evaporates because of its low boiling point (−6.6 °C), leaving behind the pre-reaction PbI_2.[19]

Although the perovskite film does not degrade in the absence of light and oxygen due to the critical step in Equation (5) above, this is not the case for $MAPbI_3$/mp-TiO_2 photovoltaics, indicating that the device interfaces may induce a different degradation mechanism than observed in thin films. In particular, the mesoporous TiO_2, which enhances the charge diffusion length in OMH-PSCs,[20] has been found to play a significant role in the degradation process[21–23] and Snaith *et al*. reported that under UV light, even encapsulated OMH-PSCs with mesoporous titanium dioxide (mp-TiO_2) suffered a rapid drop in performance compared to unencapsulated devices, which they attributed to trapped photoelectrons from the absorber layer caused by the formation of oxygen desorption surface states in the TiO_2 surface which are normally passivated in the presence of oxygen[21]

To evaluate the effect of UV light exposure we also studied the degradation process of OMH-PSCs cells with and without a covering layer of aliphatic polyurethane (TPU) containing UV absorbers with light in dry air and dry N_2 filled environments over 7 days. One device was stored in dark dry conditions to monitor any parasitic degradation effects, and it was only subjected to light for a few minutes each day to be tested. The lamps used in the aging process for both dry air and N_2 environments have a wide range of wavelengths that extend from the UV region (300 nm) to about near infrared region (800 nm). Moreover, the illumination intensity of the light used in the N_2 environment is ∼3.6 suns; therefore, one week of exposure to such light is equivalent to ∼3.6 weeks. The normalized power conversion efficiency (PCE) values of the aged samples are shown in Figure 4 (JV curves in supplementary material). The device with a UV blocking layer lost ∼35% of its initial PCE value after 7 days of continuous illumination, compared to a ∼95% loss of PCE values for the other (unshielded) device. The 35% loss in efficacy of the device with the TPU-UV blocking layer may be caused by heat coming from the lamp, which can sometimes reach ∼55 °C. However, the 60% difference in PCE loss between the devices with and without TPU is clearly caused by the UV light and its role in the interfacial degradation of the device. Devices subjected to light in dry air, both with and without TPU, lost ∼99% of their efficiency after only one day, as expected from the

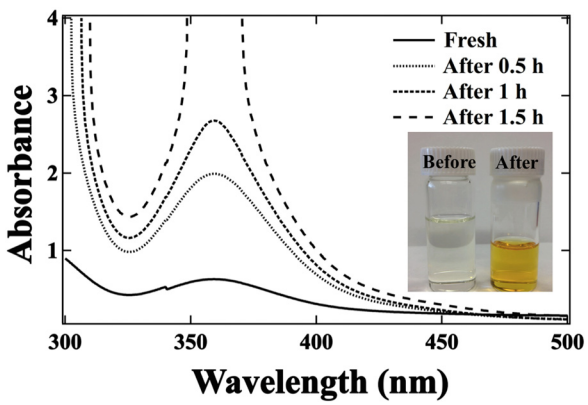

FIG. 3. The UV-Vis absorption data of MAI solution with a concentration of 10 mg/ml in isopropanol before and after illumination in air. The increase in the intensity of the peak around 365 nm indicates the release of iodine in the solution as a result of photoexcitation. The inset shows the change in the color of the MAI solution before and after illumination.

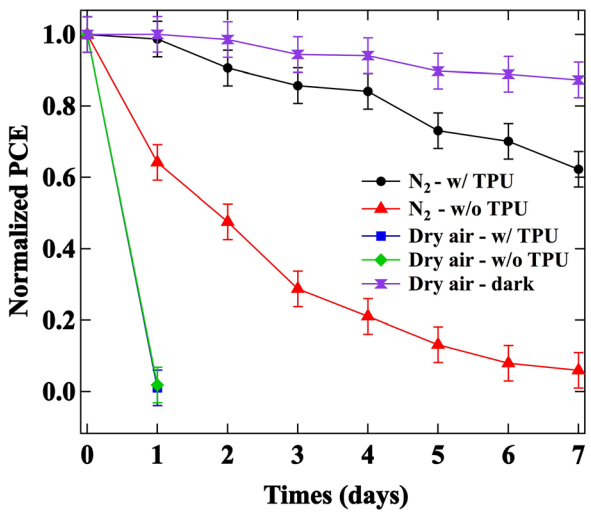

FIG. 4. Normalized power conversion efficiency (PCE) values for $MAPbI_3$/mp-TiO_2 based solar cells aged in different moisture free conditions. The performance of the solar cells was monitored with exposure to light in dry air and N_2 environments and in dark dry conditions.

degradation mechanism discussed in Equations (4)–(6). Devices stored in dark dry condition (with no TPU) for a week has lost ~10% of its efficiency attributed to degradation occurring during the light exposure during the I–V measurements.

To understand the interfacial degradation of the solar cells, the change of the local structure of $MAPbI_3$ films on mp-TiO_2 layers was studied with and without mp-TiO_2 using XRD (detailed in the supplementary material) and EXAFS. These figures plot the real part, R (fast oscillating function), of the Fast Fourier Transform (FFT) and the envelope, $\pm\sqrt{R^2+I^2}$, where I is the imaginary part of the FFT. The R functions between 4.7–5.5 Å are highly out of phase for the two materials producing destructive interference if both phases are present. Since the amplitude for PbI_2 is much larger than for $MAPbI_3$, a small amount of PbI_2 is enough to cause the phase to look more like PbI_2. In Figure 5, EXAFS data for fresh samples of $MAPbI_3$ and PbI_2 without mp-TIO_2 (top) is compared to $MAPbI_3$ degraded in light in a low humidity environment for 6 h (bottom). The shape of the phases for both traces from 4.6–5.8 Å are similar to that of PbI_2, indicating that, even in the freshest thin film $MAPbI_3$, some PbI_2 is still present. The degraded sample has an increased fraction of PbI_2, in agreement with the XRD data. To further quantify the fractions of PbI_2 present in the samples, the $MAPbI_3$ samples on mp-TiO_2 are fit using a linear combination of pure $MAPbI_3$ (fresh $MAPbI_3$ without TiO_2) and pure PbI_2 data as the standards, as described further in supplementary material. The fit results found 15% PbI_2 in the fresh $MAPbI_3$ sample on mp-TiO_2. This is greater than the 7% found by XRD, which is consistent with EXAFS being more sensitive to nanostructures than XRD, as has been shown in another study.[22,23] The fit of the data for partially degraded $MAPbI_3$ sample yields 23% PbI_2 in the sample. Since the additional PbI_2 is most likely at the interface with the mp-TiO_2, the PbI_2 may be due to the TiO_2 nanostructure shielding the deposited PbI_2 from reaction with MAI in the sequential or two-step deposition method. We note that that the remnant PbI_2 observed in our films is consistent with recent results showing that the presence of some PbI_2 improves the device performance, and our results show that widely used XRD measurement underestimates the amount of remnant PbI_2 in devices.

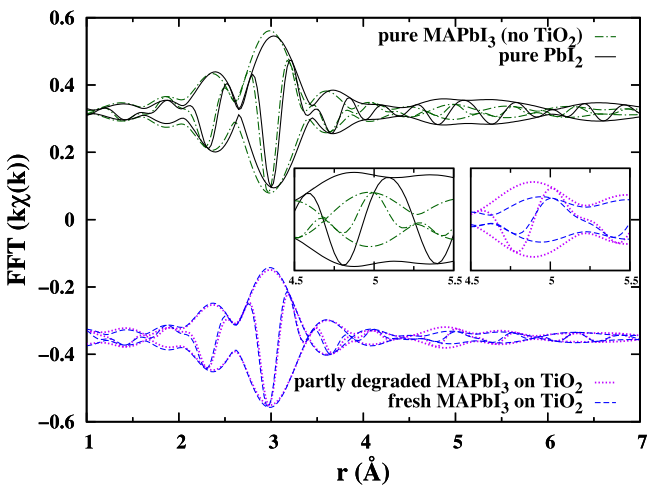

FIG. 5. Top: EXAFS data of a pure, as-prepared thin film of $MAPbI_3$ without TiO_2 and a pure, as-prepared thin film of PbI_2. These data are used as standard functions for the fit of the results on mp-TiO_2. The region of 4 Å $< r <$ 6 Å shows a significant difference between the two functions. The $MAPbI_3$ function has little amplitude and the real part is out of phase with respect to the PbI_2 function from 4.7–5.5 Å, as seen in the zoomed inset plot. Bottom: EXAFS data on thin films of fresh $MAPbI_3$ and partially degraded $MAPbI_3$, both on mp-TiO_2. In the region of 4.5 Å $< r <$ 5.5 Å, shown in the inset zoomed view, the shape of the phase indicates the presence of PbI_2 for both samples. The partially degraded $MAPbI_3$ has an increased fraction of PbI_2 content.

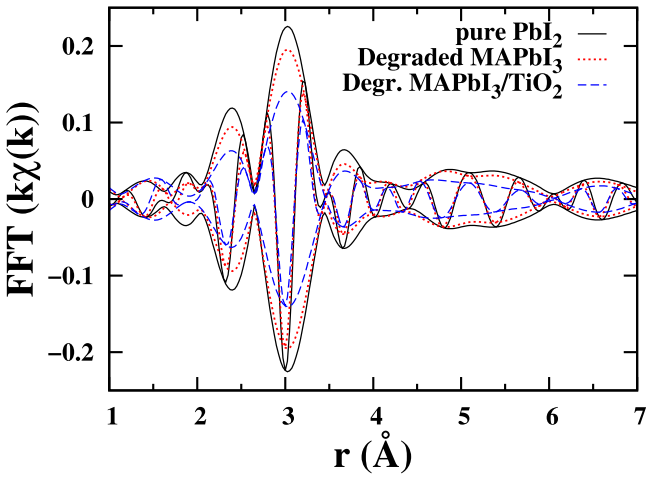

FIG. 6. EXAFS r-space data for the Pb LIII edge of fully degraded $MAPbI_3$ thin films, both without and with mp-TiO_2. The data are very similar to pure PbI_2 with an overall reduced amplitude of 87% and 63% for each, which indicates an amorphous Pb fraction of about 13% and 37% for the degraded samples without and with TiO_2, respectively.

The fully degraded $MAPbI_3$ samples look very similar to unreacted PbI_2 but with a uniform decrease in amplitude, as seen in Figure 6. The amplitude reduction is likely due to the presence of an amorphous fraction, for which a large broadening suppresses the EXAFS peaks. The term amorphous in this context refers to nanocomposite materials with a mixture of phases including other Pb compounds such as oxides. We find that degraded $MAPbI_3$ alone is 13% amorphous, while degraded $MAPbI_3$ on TiO_2 is 37% amorphous. The larger amorphous fraction for the degraded sample with TiO_2 suggests that TiO_2 accelerates the chemical reaction at the interface. These results are consistent with expectations for TiO_2, which is a known photocatalyst. TiO_2 absorbs in the UV range of light; therefore, blocking the incident UV-light greatly improves the stability of perovskite films and devices that use mp-TiO_2.

In summary, we evaluated the degradation under low humidity of $MAPbI_3$ perovskite films and devices. We found the perovskite films to be stable in oxygen in the dark and also stable under light in the absence of oxygen, but unstable under light (with and without UV) in dry air. Light exposure in air results in the oxidizing iodide anions that transfer electrons to p-type species in the atmosphere and form free radicals that react with the organic cation by capturing the acid proton, resulting in the formation of highly volatile methylamine. While the $MAPbI_3$ thin films can be made stable in a dry oxygen-free environment, perovskite/mp-TiO_2 solar cells are still unstable when exposed to UV light due to local structural changes induced by photocatalytic activity at the mp-TiO_2-$MAPbI_3$ interface.

See supplementary material for the details of device fabrication and characterizing methods, the IV curves for the solar cells under different aging conditions, and further details of XRD and EXAFS measurements related to the degradation mechanism.

This work was supported and partially funded by the Cultural Affairs and Mission Sector in Egypt and by the Bay Area Photovoltaic Consortium, DOE prime Award No. DE-EE0004946 and subaward 60965033-51077. The XRD experiments were performed by A. Durand and J. Hauser at the UC Santa Cruz X-ray Facility, supervised by S. Oliver, and funded by the NSF DMR-1126845. The EXAFS experiments were performed at SSRL, operated by the DOE, Division of Chemical Sciences. J.Z.Z. is grateful for the support from NASA (NNX15AQ01A) and UCSC Special Research Fund for financial support. We also acknowledge S. B. Naghadeh and S. A. Lindley for help with measurements.

[1]A. Kojima, A. K. Teshima, Y. Shirai, and T. Miyasaka, J. Am. Chem. Soc. **131**, 6050 (2009).
[2]W. S. Yang, J. H. Noh, N. J. Jeon, Y. C. Kim, S. Ryu, J. Seo, and S. I. Seok, Science **348**, 1234 (2015).
[3]G. Niu, X. Guo, and L. Wang, J. Mater. Chem. A **3**, 8970 (2015).
[4]J. You, Y. Yang, Z. Hong, T.-B. Song, L. Meng, Y. Liu, C. Jiang, H. Zhou, W.-H. Chang, G. Li, and Y. Yang, Appl. Phys. Lett. **105**, 183902 (2014).
[5]J. Yang, B. D. Siempelkamp, D. Liu, and T. L. Kelly, ACS Nano **9**, 1955 (2015).
[6]J. Burschka, N. Pellet, S. J. Moon, R. Humphry-Baker, P. Gao, M. K. Nazeeruddin, and M. Gratzel, Nature **499**, 316 (2013).
[7]H. Ko, J. Lee, and N. Park, J. Mater. Chem. A **3**, 8808 (2015).
[8]C. H. Booth, "R-space X-ray absorption package," see http://lise.lbl.gov/RSXAP/ (2010).
[9]C. Bi, Y. Shao, Y. Yuan, Z. Xiao, C. Wang, Y. Gao, and J. Huang, J. Mater. Chem. A **2**, 18508 (2014).
[10]A. Cabana and C. Sandorfy, Spectrochim. Acta **18**, 843 (1962).
[11]N. J. Jeon, J. H. Noh, Y. C. Kim, W. S. Yang, S. Ryu, and S. Il Seok, Nat. Mater. **13**, 897 (2014).
[12]T. Glaser, C. Müller, M. Sendner, C. Krekeler, O. E. Semonin, T. D. Hull, O. Yaffe, J. S. Owen, W. Kowalsky, A. Pucci, and R. Lovrinčić, J. Phys. Chem. Lett. **6**, 2913 (2015).
[13]N. M. Gupta, V. S. Kamble, R. M. Iyer, K. Ravindranathan Thampi, and M. Gratzel, J. Catal. **137**, 473 (1992).
[14]J. M. Gardner, M. Abrahamsson, B. H. Farnum, and G. J. Meyer, J. Am. Chem. Soc. **131**, 16206 (2009).
[15]M.-H. Zeng, Q.-X. Wang, Y.-X. Tan, S. Hu, H.-X. Zhao, L.-S. Long, and M. Kurmoo, J. Am. Chem. Soc. **132**, 2561 (2010).
[16]A. R. Leeds, J. Am. Chem. Soc. **1**(3), 65 (1879).
[17]H. A. Schwarz and B. H. J. Bielski, J. Phys. Chem. **90**, 1445 (1986).
[18]N. Aristidou, I. Sanchez-Molina, T. Chotchuangchutchaval, M. Brown, L. Martinez, T. Rath, and S. A. Haque, Angew. Chem. Int. Ed. **54**, 8208 (2015).
[19]H. D. Gibbs, J. Am. Chem. Soc. **27**(7), 851 (1905).
[20]V. Gonzalez-Pedro, E. J. Juarez-Perez, W. S. Arsyad, E. M. Barea, F. Fabregat-Santiago, I. Mora-Sero, and J. Bisquert, Nano Lett. **14**, 888 (2014).
[21]T. Leijtens, G. E. Eperon, S. Pathak, A. Abate, M. M. Lee, and H. J. Snaith, Nat. Commun. **4**, 2885 (2013).
[22]J. J. Choi, X. Yang, Z. M. Norman, S. J. L. Billinge, and J. S. Owen, Nano Lett. **14**, 127 (2014).
[23]T. J. Jacobsson, J. P. Correa-Baena, E. Halvani Anaraki, B. Phillipe, S. D. Stranks, M. E. Borduban, W. Tress, K. Schenk, J. Teuscher, J. E. Moser, H. Rensmo, and A. Hagfeldt, J. Am. Chem. Soc. **138**(21), 10331 (2016).